Effects of Thin Film Layers on Actuating Performance of Micro Heaters

Min Soo Kim, Bang Weon Lee, Yong Soo Lee, Dong Sik Shim and Keon Kuk; Micro Device & Systems Lab., Samsung Advanced Institute of Technology (SAIT); Yongin, Gyeonggi 446-712, Korea

Abstract

Effects of thin film layers have been investigated on the actuating performance of micro heaters. Bubble behaviors on micro heaters were observed experimentally, and heat conduction characteristics in thin film layers were analyzed numerically. Nine (9) kinds of tantalum nitride (TaN) micro heaters were prepared. Step-stress test (SST) showed that maximum endurable voltage levels in the non-passivated heaters are less than 50% of those in the passivated heaters. Open pool bubble test was carried out using de-ionized (DI) water as a working fluid. The non-passivated heaters could produce comparable bubbles with only 20 to 50% of the input energy required for the passivated heaters. However, the non-passivated heaters could operate only in a narrow range of driving voltage. A hybrid model for bubble nucleation was newly proposed to correlate the nucleation times obtained experimentally. The hybrid model adopts different nucleation criterion depending on the input power level. Based on the bubble work obtained from the bubble volume estimated experimentally, actuating efficiencies of micro heaters were calculated and compared. Efficiencies of the non-passivated heaters were much higher than those of the passivated heaters. However, robust actuating characteristics were difficult to obtain in a wide range of power density. Applicability of non-passivated heaters as promising micro actuators needs further investigation from the viewpoints of robustness and reliability.

1. INTRODUCTION

Micro heaters are one of the actuators widely adopted in Micro Electro Mechanical Systems (MEMS). Their material and simple structure are compatible with standard silicon process. Also, large actuating force enables the size small compared to the other types of actuators; piezoelectric, electrostatic, electromagnetic and acoustic. This is favorable for an array actuator of high spatial density such as an inkjet print head. A large number of inkjet head types have been investigated as summarized by Silverbrook **[1]**.

Various works on micro heaters contributed the understanding of the bubble generation mechanism. Asai **[2]** proposed the bubble nucleation theory to provide a guide to the design of thermal inkjet heads, and Andrews **[3]** showed the complete bubble cycles from nucleation to collapse by visualization techniques. Rembe *et al.* **[4]** visualized the non-reproducible phenomena in micro heater with real high speed cine photomicrography. Kuk *et al.* **[5]** studied the thermal efficiency of micro heaters, especially effects of heater size and aspect ratio.

In this study, effects of thin film layers have been investigated on the actuating performance of micro heaters. Bubble behaviors on micro heaters were observed experimentally, and heat conduction characteristics in thin film layers were analyzed numerically. Step-stress test and open pool bubble test were carried out. Bubble volumes were estimated from the images taken experimentally. A new hybrid model was proposed for prediction of bubble nucleation. Bubble work was calculated from the bubble volume using the pressure profile following Asai's model **[6]** as well as the nucleation pressure from heat conduction simulation. Finally, efficiencies of micro heaters with different passivation layers were obtained and compared.

2. Methods

2.1. Preparation of Micro Heaters

Micro heaters for bubble generation were fabricated using conventional MEMS technique (**Figure 1**). Thermal barrier layer of silicon dioxide (SiO_2) was thermally grown up to 3 μm on silicon wafer. Tantalum nitride (TaN) heater and Aluminum (Al) electrode were consecutively deposited by sputtering. The sheet resistance of TaN film was about 50 Ω/square. Silicon nitride (SiN_x) film was deposited using PECVD technique as a heat transfer layer. Finally, tantalum (Ta) film of 3000Å was deposited as an anti-cavitation layer.

Nine (9) kinds of micro heaters were prepared to have different thin film layers. Micro heaters had square shape and same planar size of 22 μm by 22 μm. Three (3) different thicknesses of SiO_2 were 1, 2 and 3 μm. Three (3) different types of passivation layers included non-passivation, SiN_x of 4000Å with Ta of 3000Å, and SiN_x of 6000Å with Ta of 3000Å. Heaters were arranged about 300 μm away from chip edge for bubble side view images. **Table 1** lists mean values of electrical resistance of the fabricated heaters along with their standard deviations. The number of data was sixty (60) for each case.

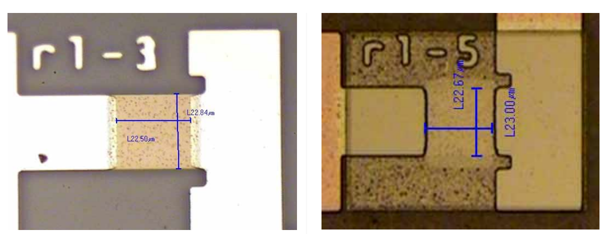

(a) (b)

Figure 1. Optical microscope images of the fabricated micro heaters; (a) Non-passivated heater; 22 μm by 22 μm micro heater with SiO_2 of 3 μm and (b) Passivated heater; 22 μm by 22 μm micro heater with SiO_2 of 1 μm, SiN_x of 6000Å and Ta of 3000Å.

Table 1. Values of electrical resistance of the fabricated micro heaters.

Passivation Type		SiO_2 1μm	2μm	3μm
No Passivation	Mean* [Ω]	60.5	64.0	59.2
	StDev [Ω]	2.2	1.3	1.0
SiN_x 4000Å & Ta 3000Å	Mean [Ω]	60.6	66.1	65.4
	StDev [Ω]	1.8	1.2	1.9
SiN_x 6000Å & Ta 3000Å	Mean [Ω]	61.0	67.6	68.6
	StDev [Ω]	1.2	1.9	1.5

* Number of samples is 60 for each heater.

Step-stress test (SST) has been performed to compare endurable voltage levels in different micro heaters. At a fixed pulse width, electrical pulse of a certain voltage level was repeatedly given to a micro heater. After 100,000 cycles at a frequency of 1 kHz, electrical resistance was measured and the driving voltage level was increased with an increment of 1V. Maximum endurable voltage was recorded as the one causing variation more than about 1% from the initial resistance.

2.2. Open Pool Bubble Visualization

Bubbles on the heaters were visualized with a microscope in an open pool setup shown in **Figure 2**. Xenon stroboscope provided sample illumination through the microscope. Bubble was synchronized with the input pulse to the heater and images of the bubble were captured by high speed CCD cameras **[7]**. Exposure time of the CCD was 0.3 μs, and frame time of the consecutive images was 0.1 μs. Estimation of the bubble volume at a fixed time requires two synchronized bubble images; plane and side views with two (2) CCD arrangements as shown in **Figure 3**. CCD1 captured the bubble width and length, and height could be obtained from the CCD2 image **[5]**.

Electrical heating pulses of square wave were applied to the micro heaters with 8 Hz repetition frequency. Heating current was measured by a current probe. Voltage difference between electrodes during pulse heating was recorded using a digital oscilloscope. Electrical power multiplied by the pulse width represents input energy to the heater **[8]**.

Bubble volume was calculated as a function of time through elaborating image processing with both plane and side views of bubbles taken experimentally **[5]**. Work of bubble formation was estimated with Asai's pressure model **[2, 6]** following the procedure in **[5]**.

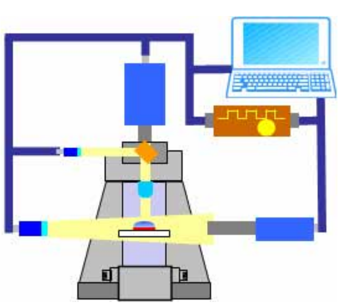

Figure 2. Experimental setup for open pool bubble visualization.

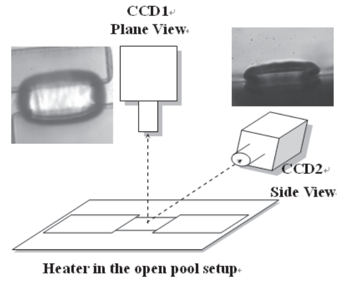

Figure 3. Two CCDs for capturing both plane and side views of bubble.

2.3. New Hybrid Model on Bubble Nucleation

In the present study, three models for bubble nucleation were compared with experimental data. In the temperature criterion model, bubble starts to nucleate when the maximum temperature at the interface between heater and fluid reaches a specific temperature. In the heat flux model **[9]**, the criterion temperature (T_{cri}) is determined considering heat flux through the interface in stead of the interfacial temperature as follows;

$$T_{heat} = 230\,°C + L_{char} \frac{\partial T}{\partial z}, \tag{1}$$

where T_{heat} is T_{cri} for the heat flux model, and L_{char} is the thermal characteristic thickness of the heat flux model.

However, these two models showed agreement with experimental data only in a specific range of power density. In the present study, a hybrid model for bubble nucleation was newly proposed. In the hybrid model, the shorter nucleation time was adopted between two nucleation times by the temperature model and the heat flux model as follows;

$$t_{hybrid} = \mathrm{MIN}\ [t_{temp}, t_{heat}], \tag{2}$$

where t_{temp} represents the nucleation time determined by the temperature model and t_{heat} by the heat flux model.

The criterion temperature and the thermal characteristic thickness of the heat flux model were determined by comparing numerical results with experimental data for the case of 4000Å SiN_x and 3 μm SiO_2. In the present study, the values were chosen as T_{cri} = 360°C and L_{char} = 0.2 μm.

Numerical analyses of heat transfer in thin film layers have been performed using CFD-ACE v2004 for 7 different heaters; three (3) non-passivated heaters with thermal barrier (SiO_2) thickness of 1, 2 and 3 μm, and four (4) passivated heaters with passivation layer (SiN_x) thickness of 4000 and 6000Å, each having two (2) different thermal barrier (SiO_2) thicknesses of 1 and 3 μm.

3. Results and Discussions

3.1. Step-Stress Test of Micro Heaters

For different passivation types, **Figure 4** depicts maximum endurable voltage levels at several selected pulse widths. Thermal barrier thickness (SiO_2) was fixed with 1 μm. For a specific passivation type, higher voltage could be used with shorter pulse width. Maximum voltage levels of the passivated heaters were about two times higher than those of the non-passivated heaters. For example, at a pulse width of 1 μs, maximum voltage was 5 V for the non-passivated heater while 13 V for the passivated heater with SiN_x 6000Å and Ta 3000Å. Also, the heater with thicker passivation layer could stand higher voltage. On the other hand, the non-passivated heater had a narrow range of driving voltage compared to the passivated heaters.

Table 2 shows voltage limits of nine (9) micro heaters at 1 μs pulse width. Voltage limits were higher for thicker passivation layers. On the other hand, effects of thermal barrier thickness on the voltage limits seem to appear with increasing thickness of passivation layer. In the present study, the highest voltage limit was obtained for the micro heater of the thickest passivation layer with the thinnest thermal barrier layer.

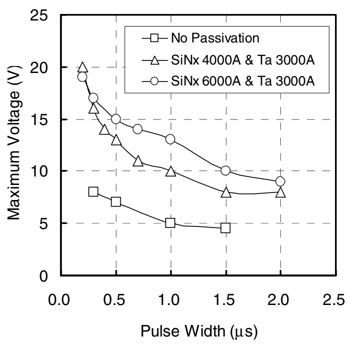

Figure 4. Results from step-stress test of micro heaters, presenting maximum endurable voltage levels as a function of pulse width for three (3) different passivation types.

Table 2. Maximum voltages at 1 μs pulse width for three (3) different passivation types, each having three (3) different thicknesses of thermal barrier layer (SiO_2).

	SiO_2		
	1μm	2μm	3μm
No Passivation	5	5	5
SiN_x 4000Å & Ta 3000Å	10	9	9
SiN_x 6000Å & Ta 3000Å	13	9	10

3.2. Driving Conditions for Bubble Actuation

Figure 5 depicts relations between driving voltage and pulse width for bubble creation on the micro heaters with different passivation layers. Again, thermal barrier thickness (SiO_2) was fixed with 1 μm. For the non-passivated heater, available driving voltage margin was relatively small. Also, at a fixed pulse width, optimal bubble was observed with a driving voltage near the voltage limit obtained from SST. However, the passivated heaters could produce stable bubbles far below the voltage limit. On the other hand, at a fixed driving voltage, longer pulse width was required for the heater with thicker passivation layer to produce stable bubbles. This means that more input energy should be provided to the heaters with thicker passivation layers. The prescribed thermal energy should be transferred to fluid for normal bubble creation.

Input energy for normal bubble creation is plotted in **Figure 6**. In the non-passivated heaters, input energy of about 20 to 50% was consumed for normal bubble creation as compared to the passivated heaters. More energy was required for heaters with thicker passivation layers. Experiments showed that input energy decreases with increasing driving voltage, i.e., with increasing driving power. For passivated heaters, input energy seemed to saturate after around 9 V, while non-passivated heaters showed no saturation region, possibly due to the narrow range of driving voltage.

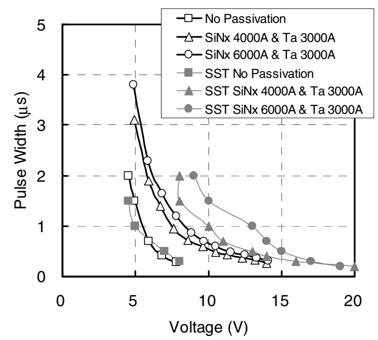

Figure 5. Driving conditions of micro heaters of different passivation types for normal bubble creation, along with corresponding SST results.

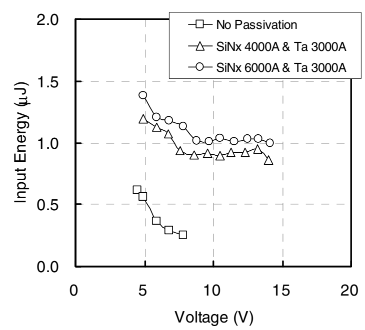

Figure 6. Input energy to micro heaters of different passivation types at the normal bubble creation.

Characteristics of bubble creation are described in **Figure 7**. The bubble nucleation time is depicted in **Figure 7a** and bubble life in **Figure 7b**. Open pool bubble test might have a system delay of about 0.1 μs between trigger signal and actual heating pulse to the micro heater. Therefore, the obtained nucleation time has an uncertainty of the corresponding error. The nucleation time was dependent largely on the driving power. Higher driving power resulted in earlier bubble nucleation. At the same driving power, faster bubble nucleation was observed on the non-passivated heaters. On the other hand, the created bubbles lasted longer on the passivated heaters. Bubble life decreased with increasing driving power. Thickness of passivation layers seemed to make little difference in bubble life.

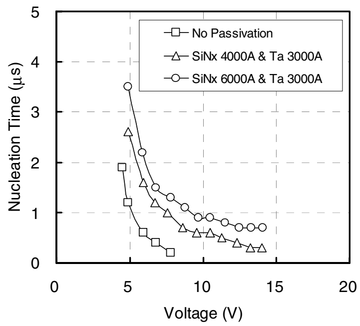

(a)

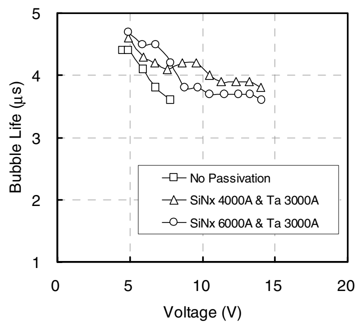

(b)

Figure 7. Bubble characteristics; (a) Bubble nucleation time and (b) Bubble life for three (3) different passivation types.

3.3. Bubble Nucleation, Bubble Work and Actuating Efficiency

With the values of T_{cri} = 360°C and L_{char} = 0.2 µm obtained in **Section 2.3**, the hybrid model predicted nucleation time in good agreement with experimental data as shown in **Figure 8**. The temperature model agreed partially in high power density, while the heat flux model agreed partially in low power density. However, the prediction from the hybrid model provided excellent agreement with experiments in the whole range of power density.

The energy provided till the nucleation time was calculated and shown in **Figure 9a**. For the non-passivated heaters, the input energy decreased about 50% when the power density changed from 0.8 to 2 GW/m^2. However, for the passivated heaters, the input energy was affected little by the change of power density. As shown in **Figure 9b**, the energy transferred to fluid till the nucleation time was reversely proportional to the power density for both non-passivated and passivated heaters.

The estimated bubble work and efficiency are presented in **Figure 10**. Bubble work decreased with increasing power density for all passivation types as shown in **Figure 10a**. This might be explained by smaller bubble size and shorter bubble life along with less heat transfer to fluid due to earlier nucleation for higher power density. Results also show that comparable bubble work can be produced from the non-passivated heaters. This indicates that the non-passivated heater meets one basic nature as an actuator. For passivated heaters, thickness of passivation layer (SiN_x) affected both bubble work and efficiency. The heaters with 4000Å SiN_x produced more bubble work showing higher efficiency than those with 6000Å SiN_x at the same power density.

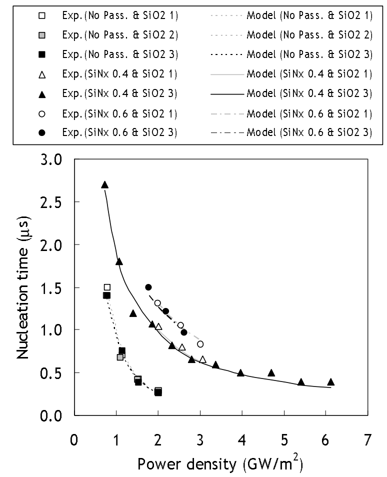

Figure 8. Prediction of nucleation time from the hybrid nucleation model along with the corresponding experimental data in Figure 7a.

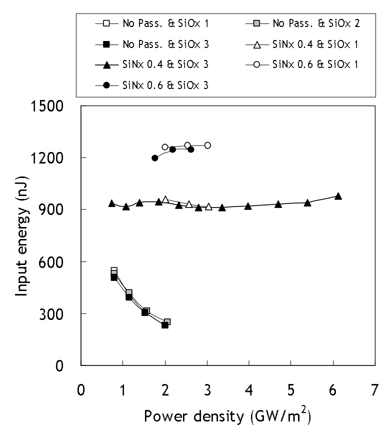

(a)

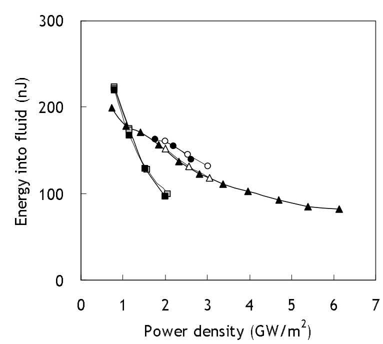

(b)

Figure 9. Simulation results based on the hybrid nucleation model; (a) Input energy till the nucleation time and (b) Effective energy transferred to fluid for different thin film layers.

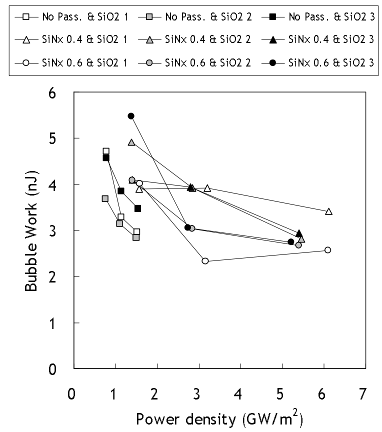

(a)

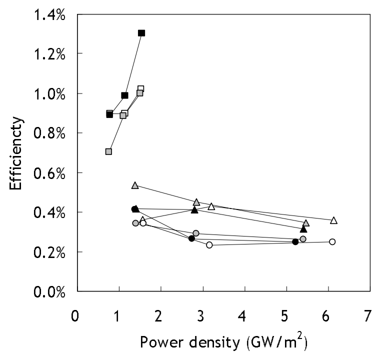

(b)

Figure 10. (a) Estimated bubble work and (b) Actuating efficiency defined as a ratio of bubble work to the input energy.

On the other hand, in the power density range of about 1 to 2 GW/m^2 in **Figure 10b**, the non-passivated heaters showed much higher efficiency although they produced less bubble work. From **Figure 9**, the non-passivated heaters could deliver about half the input energy to fluid. In the power density less than 1 GW/m^2, the non-passivated heater could transport about 12% more energy into fluid compared to the passivated heaters even with less input energy. Therefore, the non-passivated heaters could produce comparable bubble work with less input energy in the lower power density. This strongly supports higher efficiency of the non-passivated heaters in **Figure 10b**.

Besides, in **Figure 10b**, efficiency of the non-passivated heaters showed the opposite trend when increasing power density. This could be explained by the non-linear effect of the passivation layers on the heat transfer from heater to fluid. As power density increases, in the passivated heaters, temperature gradient at fluid interface is kept almost constant due to existence of the passivation layers, while it increases accordingly for the non-passivated heaters. From **Figure 8**, higher power density results in earlier bubble nucleation, showing much larger decreasing rate for the case of non-passivated heaters. This implies that relatively large decrease in input energy is caused for the non-passivated heaters, which is confirmed in **Figure 9a**. Earlier nucleation means decrease in heat transfer time for transporting thermal energy to fluid. However, for the non-passivated heaters, effective energy transferred to fluid is affected little due to no energy storage in the passivation layers as in the passivated heaters. Thus, the prescribed thermal energy for bubble creation can be delivered to fluid with much less input energy (**Figure 9**). Also, bubble work is roughly proportional to the energy into fluid (**Figure 10a** and **Figure 9b**). Therefore, the actuating efficiency, defined as a ratio of bubble work to the input energy, increases with increasing power density for the non-passivated heaters.

4. Conclusions

Results from step-stress test emphasize that maximum power density level for the non-passivated heater should be kept low compared to the passivated heaters. Open pool bubble actuation indicates that energy margin is very small for the non-passivated heaters. On the contrary, the non-passivated heaters showed much higher actuating efficiency even with less input energy, but only in the limited range of power density. Also, the hybrid model could predict nucleation time in excellent agreement with experimental data. Applicability of non-passivated heaters as promising micro actuators needs further investigation from the viewpoints of robustness and reliability. Our investigation will be helpful for development of the thermal inkjet heads of more reliable and higher performance.

References

[1] K. Silverbrook, **US Patent 6,338,547 B1** (2002).
[2] A. Asai, **Jpn. J. Appl. Phys.**, 28(5), 909-915 (1989).
[3] J. R. Andrews, **IMA Workshops**, Minneapolis, MN (IMA, Cambridge, UK, 2001).
[4] C. Rembe, S. Wiesche, M. Beuten, and E. P. Hofer, **Proc. SPIE 3409**, 316-325 (1998).
[5] K. Kuk, J. H. Lim, M. S. Kim, M. C. Choi, C. H. Cho, and Y. S. Oh, "Research on Micro Heater Efficiency for Thermal Inkjet Head," **J. of Imaging Science and Technology**, 49(5), 545-549 (2005).
[6] A. Asai, "Bubble Dynamics in Boiling under High Heat Flux Pulse Heating," **J. of Heat Transfer**, 113, 973-979 (1991).
[7] C. Rembe, J. Patzer, E. Hofer, and P. Kreh, **J. of Imaging Science and Technology**, 40(5), 400-404 (1996).
[8] J. H. Lim, Y. S. Lee, H. T. Lim, S. S. Baek, K. Kuk, and Y. S. Oh, **Proc. IEEE MEMS Conference**, 197-200 (IEEE, Piscataway, NJ, 2003).
[9] W. Runge, "Nucleation in Thermal Ink-Jet Printers," **IS&T's Eighth International Congress on Advances in Non-Impact Printing Technologies**, 299-302 (1992).

Author Biography

M.S. Kim received his Ph.D. degree in Mechanical Engineering from Seoul National University (SNU), Seoul, Korea in 1998. After one and half year as a post-doctoral research fellow at Kyoto University (KU), Kyoto, Japan, he joined Samsung Electronics Co. Ltd. (SEC), Korea in 2000, and has been with Samsung Advanced Institute of Technology (SAIT), Korea since 2001. His scientific interests include micro thermo-fluidics, inkjet printing and MEMS.